Experimental Mechanics (2020) 60:679–694
https://doi.org/10.1007/s11340-020-00591-8

RESEARCH PAPER

Acoustic Emission Source Localization with Generalized Regression Neural Network Based on Time Difference Mapping Method

Z.H. Liu [1,2] · Q.L. Peng [1,2] · X. Li [1,2] · C.F. He [1,2] · B. Wu [1,2]

Received: 11 March 2019 / Accepted: 20 February 2020 / Published online: 2 March 2020

Abstract

Acoustic emission (AE) source localization is a powerful detection method. Time Difference Mapping (TDM) method is an effective method for detecting defects in complex structures. The core of this method is to search for a point with the minimum distance away from the verification point in the time difference database. In Traditional Time Difference Mapping (T-TDM) method and Improved Time Difference Mapping (I-TDM) method, the larger database and denser grids allow the higher localization accuracy. If the location points are not included in the database, the localization accuracy of the T-TDM and I-TDM methods will be greatly affected. To solve the above problems, a new AE source localization method, Generalized Regression Neural Network Based on Time Difference Mapping (GRNN-TDM), is proposed to improve the localization accuracy in the study. In the proposed method, the time difference data of the sensor path on all nodes in the time difference mapping are used as the training input data and the coordinates of grid nodes are used as the training output data. After continuous learning and training, the neural network model predicts its possible source location with the time difference data collected from the verification point. In this paper, the localization of AE sources with T-TDM, I-TDM and GRNN-TDM methods was studied in four composite plates with different fiber layers and an aluminum plate with holes. The localization results showed that the localization accuracy of the GRNN-TDM method was higher than that of T-TDM and I-TDM methods.

Keywords Time difference mapping method · Generalized regression neural network · Acoustic emission · Composite plate · Structural health monitoring

Introduction

Structural health monitoring (SHM) refers to the process involving structural assessment, performance monitoring, and damage detection. The early detection of damage and proper modifications can prevent structural failures, reduce maintenance and replacement costs, and ensure the safe and effective operation [1–4]. As one of SHM methods, Acoustic emission (AE) technology can detect early cracks and monitor engineering structures. AE is a nondestructive testing method based on the passive dynamic measurement of a structure. AE is sensitive to dynamic defects and has its unique characteristics, such as real-time dynamic monitoring [5]. It has the wide application potential in real-time monitoring of in-service plate-like structures. TDM method is a new AE source localization method proposed by Baxter et al. [6] and has the good application potential because it does not need to consider the propagation speed of waves or different modes and can quickly and accurately localize the sound source in a structure.

The localization accuracy of AE source is an important index of AE detection. It is necessary to improve the accuracy of acoustic source localization and minimize the influences of interference factors such as missing location and pseudo location in AE detection [7, 8]. The traditional AE localization method is a time-of-arrival (TOA) method. In complex structures, the propagation velocity of acoustic waves varies with the propagation angle. The TOA method requires the structural homogeneity and the consistent wave velocity in all the directions. Therefore, the TOA method cannot accurately localize defects in complex structures. Many researchers attempted to improve the accuracy and reliability of AE source localization.

✉ Z. H. Liu
liuzenghua@bjut.edu.cn

[1] College of Mechanical Engineering and Applied Electronics Technology, Beijing University of Technology, Beijing 100124, China

[2] Beijing Engineering Research Center of Precision Measurement Technology and Instruments, Beijing University of Technology, Beijing 100124, China

Mhamdi et al. [9] proposed a phased array method for predicting the location of AE sources in a steel plate and more accurately determined the direction and spatial position of AE sources than the traditional arrival time method. Kundu et al. [10–12] localized acoustic source without any knowledge of the plate material properties or the direction-dependent velocity distribution in the plate. A clustering algorithm was used in sensors to calculate the location of AE source and explore the localization theory of AE sources in different materials, the AE source localization algorithm and localization principle for different materials, but there was a certain deviation between experimental results and actual source locations. Park et al. [13] introduced a technique to localize the acoustic source in a highly anisotropic plate that generated rhombus and elliptic wave fronts. Sen et al. [14, 15] extended this concept and considered more non-circular wave fronts. The wave front shape-based source localization techniques proposed by Park et al. [13] and Sen et al. [14] avoided the assumption of the straight-line wave propagation path from the acoustic source to the sensor. Simone et al. [16] proposed a novel monitoring system which allowed the linearization of well-known nonlinear system of equations for the estimation of the impact location with the aid of four receiving sensors. Ebrahimkhanlou and Salamone [17] proposed a single-sensor approach based on edge reflections in an isotropic plate and a deep learning method of plate structures. Ebrahimkhanlou et al. [18] introduced a deep learning-based framework to localize and characterize AE sources in plate-like structures with complex geometric features, such as doublers and rivet connections. Liu et al. [19] calculated the delay of the multichannel AE signal with the time reversal algorithm and A_0 mode and realized the localization of AE sources in a steel plate with the sensor array.

James et al. [20] used feed-forward neural networks to localize AE sources. Even in isotropic material structures, there is an inconsistency in the speed of AE signals in different propagation directions. Different AE source localization algorithms and theories have different application conditions and scopes and the accuracy and precision of AE source localization should be improved.

However, the changes in the wave propagation path or wave velocity caused by some factors such as a hole and thickness change in a structure are not considered in these methods.

Eaton et al. [21] used the TDM method to localize the AE source in fiber-reinforced composite plates. They collected AE signals from grids through pencil lead break (PLB), processed the data with the interpolation method, and obtained accurate and stable source localization results.

In this study, based on T-TDM and I-TDM methods, GRNN-TDM acoustic source localization method is proposed. The rest of the paper is organized as follows. Section 2 mainly introduces the technical principle and steps of T-TDM and I-TDM methods. The steps and main features of the GRNN-TDM method proposed in this paper are introduced in Section 3. Section 4 introduces the experimental arrangement. Section 5 gives the experimental results and analysis results. In four kinds of composite plates with different fiber layers and an aluminum plate with holes of different diameters, the locations of AE sources were predicted by T-TDM, I-TDM and GRNN-TDM methods in this study. The conclusion is drawn in Section 6.

Technical Principles

Traditional Time Difference Mapping (T-TDM) Method

TDM method is a coverage mapping technique and mainly localizes a defect through selecting the path in the time difference contour map. The time difference contour map of different paths is firstly plotted with AE signals generated by a defect and then the consistent time difference in the error range is calculated to determine the actual AE event location. The time difference training map database created by this method is obtained from the entire detection area. Therefore, it is not required to consider the influences of defects, thickness variations, or complex geometries in the detection area. In the TDM method, it is not necessary to consider the propagation speed of the wave in materials, the dispersion information or the mode of Lamb waves. The T-TDM method is mainly based on the methods proposed by Baxter et al. [6] and involves the following five steps:

Determination of the Area to Be Detected

The TDM method belongs to the regional detection technology and can localize defects in the detection area. The sensitivities of the stresses in different regions of plate structures to the defects are different, so the detection area should be determined before the detection in order to ensure the consistency of the experimental process.

Division of Time Difference Training Grids

Time difference training grids are divided in the detection area determined above. The size of the training grid in the detection area directly determines the localization accuracy of the source. The higher the resolution of the training grid is, the higher the localization accuracy of TDM source is. However, the minimum size resolution of the training grid should be no less than one wavelength. The location of the AE source is determined by the time difference training grid divided in the specimen structure and independent of the sensor arrangement.

Acquisition of Arrival Time Data

Artificial PLB [22] is used to simulate the grid at each node and obtain the time information of AE signals arriving at the sensor. To ensure the accuracy of experimental data and reduce the errors in the training data source, each node needs repeated PLB to provide an average result. For complex geometric structures, it is not required to collect the data at every node in the grid or increase the grid density. Missing data points can be compensated by interpolation algorithms.

Calculation of Time Difference Maps

According to the arrival time data of each sensor on each node acquired above, the arrival time difference of each sensor path is calculated. For example, if four sensors are arranged in an experiment, six pairs of sensor paths will be generated: 1–2, 1–3, 1–4, 2–3, 2–4 and 3–4 paths. The time difference data of each pair of paths are averaged and then contour maps, also called time difference mapping map, are generated with the average of the time differences of all the paths.

Comparison with Actual AE Data

The differences between the time difference data of the six pairs of sensor paths of the actual AE event and the data in the training time difference mapping database are calculated. Each time difference can be used to select the possible points of the AE source from the time difference contour map drawn above. The contour lines of each path are superimposed to determine the convergence point. In theory, the intersection point of the six paths cross the location of the AE source. In fact, due to the discreteness of the data, all lines do not intersect at the same point. Therefore, a weighted mathematical algorithm [6] is used to determine its possible source location.

Improved Time Difference Mapping (I-TDM) Method

Although the T-TDM method can localize acoustic sources, there are still many problems. In the above steps, it is necessary to collect a lot of arrival time data of AE events on each grid node. In the data acquisition process, operation errors inevitably lead to abnormal data. In addition, it is necessary to select an appropriate cluster diameter for validating the location of actual AE events, but the optimal cluster diameter varies with the position.

To reduce the errors of T-TDM method, I-TDM method is proposed. The method involves two main parts. Firstly, an unsupervised clustering method is used to select correct AE events to eliminate the abnormal data caused by artificial or environmental factors. Secondly, the minimum difference method [23] is used to calculate the location of the AE source.

Selection of Correct AE Events

To select correct AE events for generating a time difference training map, the system clustering analysis method is used to select the AE events on each grid node in the map. System clustering is a clustering method which minimizes the distance between all vectors and the center of data set. With the sum of squared errors as the clustering criterion, the algorithm optimizes the clustering results through multiple iterations in order to minimize the square sum of the distance of all the samples to the center of their own category. From All N AE events collected on all grid nodes, correct AE events are obtained with the above algorithm.

The complete link hierarchical clustering algorithm for N AE events data is described in the following steps:

Step 1. The Euclidean distance between every two N events is calculated.

Step 2. The calculated Euclidean distance is classified and sorted step by step according to the size and the events with Euclidean distance value greater than the specified threshold are removed.

Step 3. The events obtained after removing the error is treated as a class to calculate its centroid, which is taken as a correct AE event.

In this study, the correlation coefficient of 0.99 is chosen as the screening threshold in data filtering and all events in this group were used (correlation coefficient of 1 means total correlation). Each group at this level or above is deemed to contain highly correlated events and used for onward analysis. Conversely the groups are deemed to be suitably less correlated at a correlation level lower than the highest level. So, they are ignored and not used for onwards analysis. The N AE event data collected on each grid point are screened according to the above algorithm to obtain correct AE events, thus optimizing the experimental data in the whole process. Pseudo AE events refer to the data caused by factors such as human or environmental factors during the acquisition process, rather than the data obtained by the PLB method. Correct AE events refers to acoustic emission data caused by PLB method. To more clearly display the data analysis process of the collected data containing pseudo AE events and correct AE events (the specific experimental setup and experimental conditions are described in Section 3), Fig. 1 shows a dendrogram of cluster analysis. Figure 1a shows a dendrogram of eight clustering data collected from a grid node with pseudo AE events. It can be seen that the eighth data collected in the eight AE events have larger anomalies and can be automatically identified and deleted by the clustering algorithm. Figure 1b

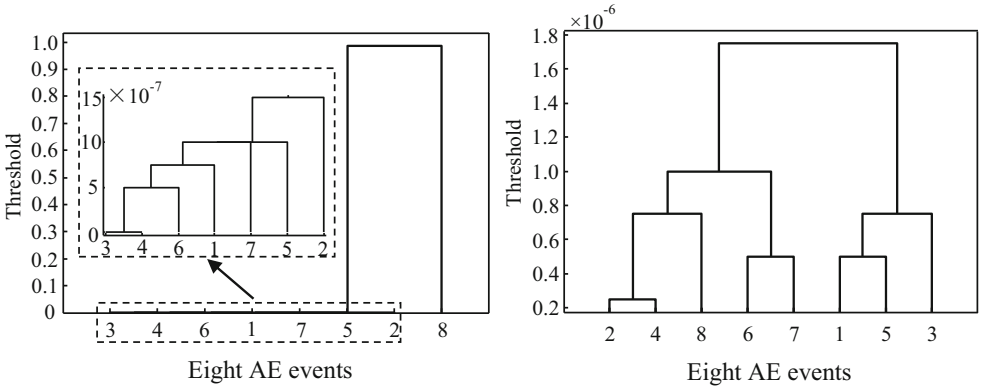

Fig. 1 Cluster analysis tree diagram

(a) Data containing pseudo AE events.

(b) Data of correct AE events.

shows the data analysis of correct AE events, which can be divided into three categories: verification points 2, 4 and 8, verification points 6 and 7, and verification points 1, 5, and 3.

Figure 2 shows a screened and compensatory mapping map of AE events. Clustering algorithm was used to remove the abnormal data caused by artificial or environmental factors. Figure 2a shows a training database of all the screened time differences of the sensor path of 1 to 2. To obtain a complete time difference training database, the surface fitting algorithm was used to compensate the missing data in the graph. The compensated results are shown in Fig. 2b. The compensated time difference database can better reflect the propagation of AE source in the plate.

The data of other time difference paths were compensated by the same algorithm. Finally, a complete time difference training mapping database was obtained and then the corresponding algorithm was used to verify the actual AE events through AE source location.

AE Source Localization through the Minimum Difference Method

Minimum difference method is a numerical method of searching for the point where the difference between the actual source data and the training map data is minimized. The minimum difference method is performed into the following steps:

Step 1. To calculate the arrival time difference between each AE event and each pair of sensors.

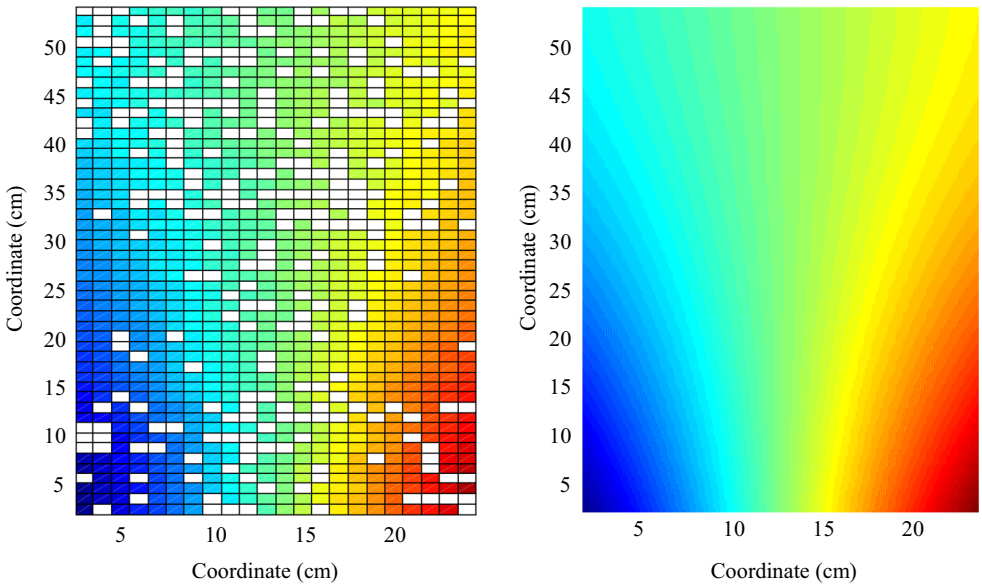

Fig. 2 Screening and compensation map of AE events

(a) Database generated by deleting the pseudo AE events

(b) Database generated by the compensation algorithm

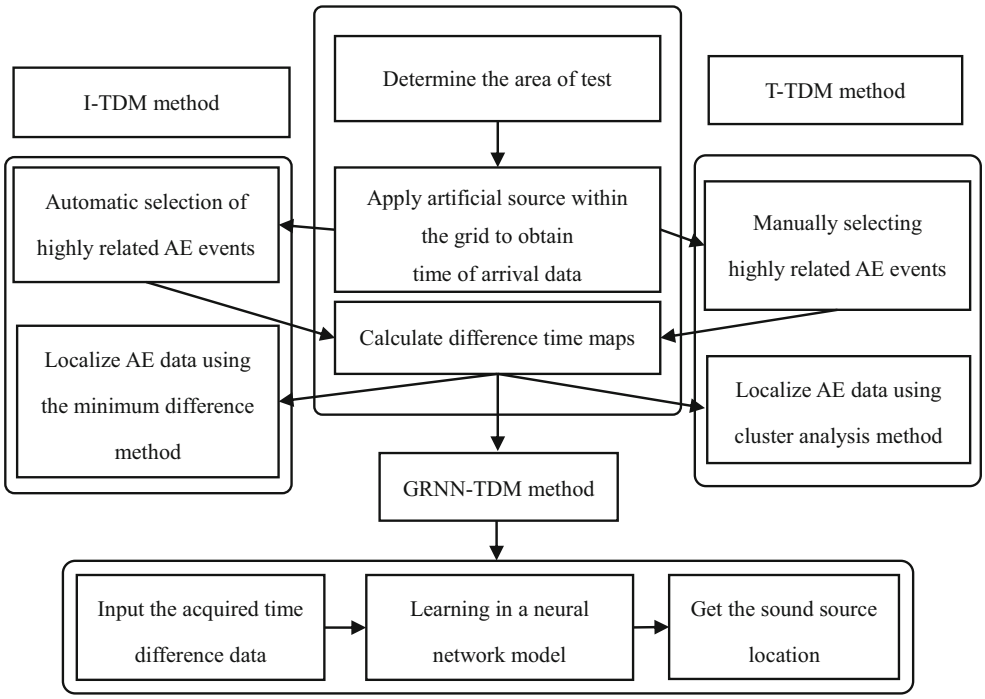

Fig. 3 Flow chart of the comparison between TDM, I-TDM and GRNN-TDM methods

Step 2. To obtain the distance between AE source and training mapping data by subtracting the arrival time difference of each sensor path in training mapping data from that of each sensor path.

Step 3. To calculate the distance between sensor paths n of all sources according to Eq. (1). The minimum difference method is used to search for the point where the difference between the actual source data and the training map data is minimized, and the obtained point is the location of the AE source. The calculation formula is as follows:

$$S = \sum_{1}^{n} \left| T_{source} - T_{mapping\,map} \right|, \tag{1}$$

where S is the sum of the time differences between the six sensor paths of the AE source verification point and the training data; T_{source} is the time difference of the AE source;

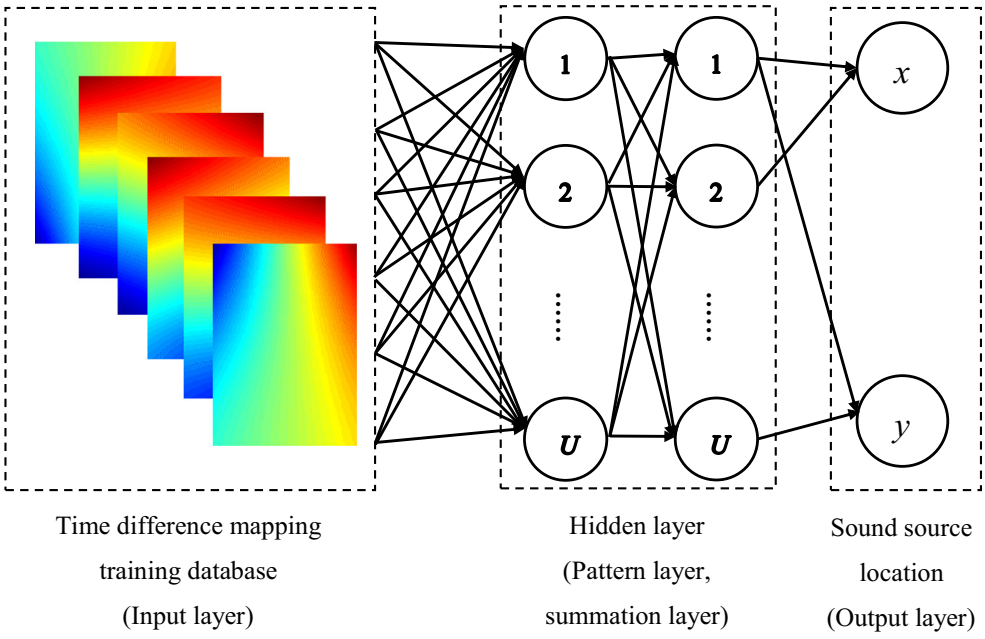

Fig. 4 Schematic diagram of AE source localization of the GRNN-TDM method

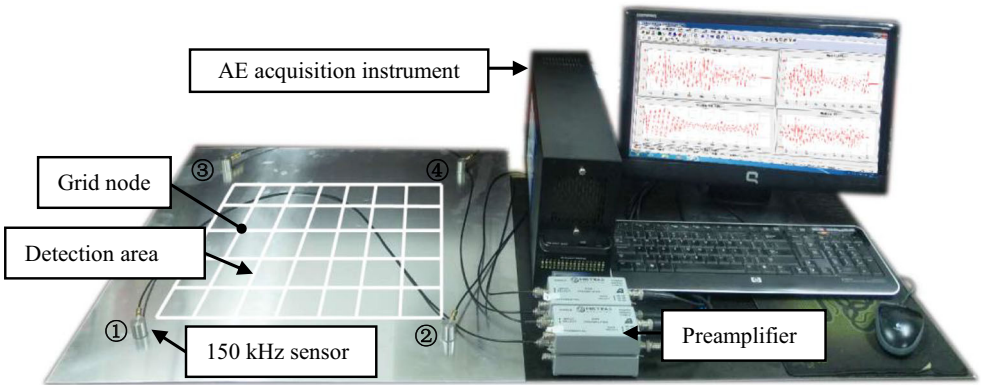

Fig. 5 Picture of the AE experimental system

$T_{\text{mapping map}}$ is the time difference of all AE events in training mapping maps.

The minimum difference method is used to verify the location of AE source at actual AE verification points. The method can avoid the artificial interference in the calculation process and the selection of cluster diameter for different sources, reduce the source of errors, improve the reliability of the results, shorten the running time of the whole process, and improve the localization accuracy and precision.

AE Source Localization with Generalized Regression Neural Network Based on Time Difference Mapping (GRNN-TDM) Method

The main idea of the T-TDM and I-TDM methods is to find the point with the smallest distance away from the verification point in the time difference database. If the density of the drawn grids is denser, the database is larger and the localization accuracy is higher. The interpolation algorithm is required. If the location point is not included in the database, the localization accuracy of the T-TDM and I-TDM methods is greatly affected. To reduce the workload and improve the localization accuracy of the source and the generalization of the method, GRNN-TDM method is proposed. The comparison between T-TDM, I-TDM and GRNN-TDM methods is illustrated in Fig. 3.

GRNN is a radial basis neural network and has the strong nonlinear mapping capability, flexible network structure and high fault tolerance and robustness. It is applicable to solve nonlinear problems. The prediction accuracy is also relatively high when the sample size is small. The GRNN network can also process unstable data. The algorithm breaks through the linear limitation of traditional parameter processing. With the good learning ability and highly nonlinear mapping characteristics, it can be used in the localization of AE sources in complex materials and structures. The GRNN consists of four layers: the input layer, the pattern layer, the summation layer, and the output layer. Figure 4 shows the AE source localization structure of the GRNN-TDM method.

The number of input layer neurons is equal to the dimension of the input vector in the learning sample, namely, the time difference of the six pairs of paths. Each neuron is a simple distribution unit which passes the input variables directly to the pattern layer. The number of pattern layer neurons is equal to the number of learning samples, n. Each neuron corresponds to a sample. The transfer function of the neurons of the pattern layer is expressed as:

$$p_i = \exp\left[-\frac{(X-X_i)^T(X-X_i)}{2\sigma^2}\right], i = 1, 2, ..., n, \tag{2}$$

where p_i is the exponential form of the square of the Euclidean distance between the input variable and the corresponding sample X; X is network input variable; X_i is the learning sample corresponding to the i-th neuron.

The summation layer uses two types to weight the summation of neurons in all pattern layers. The number of neurons in the output layer is equal to the dimension of the output vector in the learning sample. In each neuron, the weighted output of the summation layer is divided by the arithmetic output of the

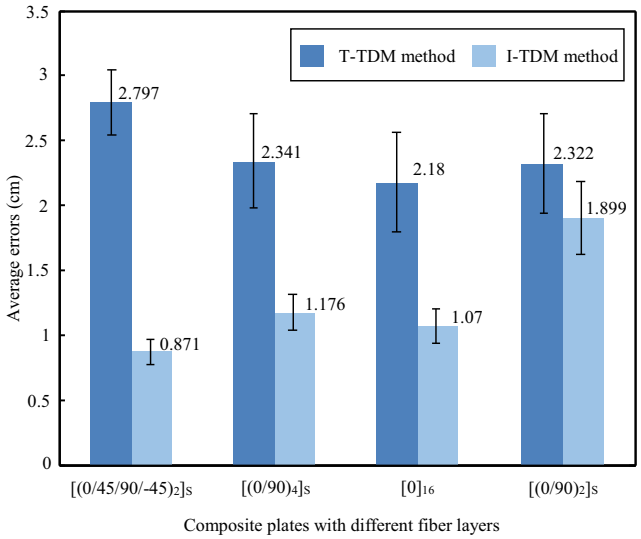

Fig. 6 Average localization errors in four kinds of composite plates of two methods

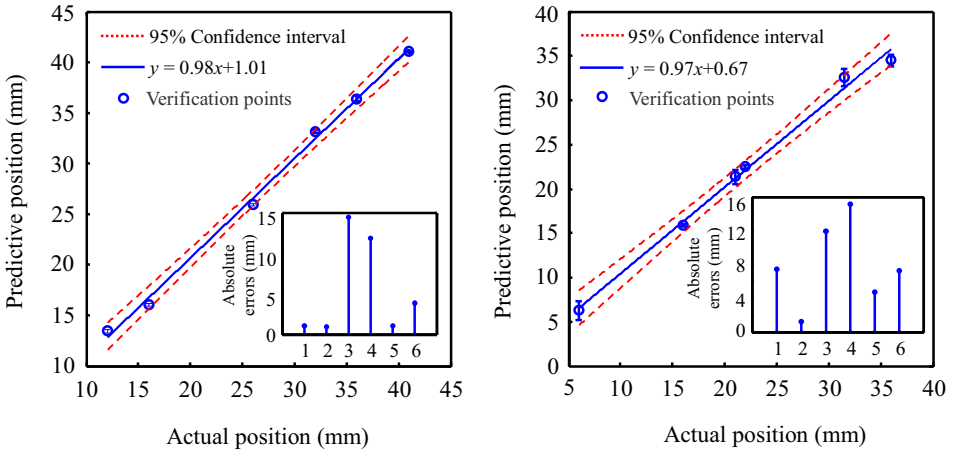

(a) Prediction results of the x coordinates of the verification points

(b) Prediction results of the y coordinates of the verification points

Fig. 7 Linear regression results of six verification points in $[0]_{16}$ fiber laminates

summation layer and the output of the neuron is the predicted position of the AE source in the detection structure. The theoretical basis of the GRNN network is nonlinear regression analysis. The regression analysis of the dependent variable Y with respect to the independent variable x is to calculate the y which has the largest probability value. Let the joint probability density function of the random variables x and y be $f(x, y)$. It is known that the observed value of x is X, then the regression of y with respect to X, the conditional mean, is calculated as:

$$\widehat{Y} = E\left({}^{y}/_{X}\right) = \frac{\int_{-\infty}^{\infty} yf(X,y)dy}{\int_{-\infty}^{\infty} f(X,y)dy}, \tag{3}$$

where $\widehat{Y}$ is the predicted output of Y when the input is X.

The time difference data of sensor paths on all the nodes in the time difference map are used as the training input data and the coordinate of corresponding node is used as the training output data. After continuous learning and training in the neural network model, the time difference data collected with the verification point can be used to predict the possible location of AE source.

Experimental Arrangement

AE source localization of the GRNN-TDM method was experimentally explored with four differently laminated composite plates and an aluminum plate with holes. As shown in Fig. 5, the experimental system is composed of the PCI-DSP 16-channel AE signal acquisition instrument (including the monitor), four AE sensors with a resonant frequency of

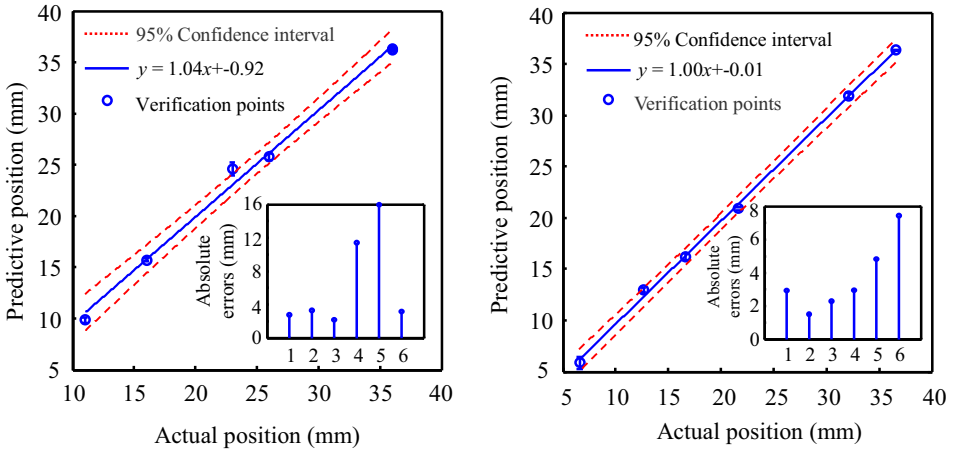

(a) Prediction results of the x coordinates of the verification points

(b) Prediction results of the y coordinates of the verification points

Fig. 8 Linear regression results of six verification points in $[0/45/90/-45]_{2s}$ fiber laminates

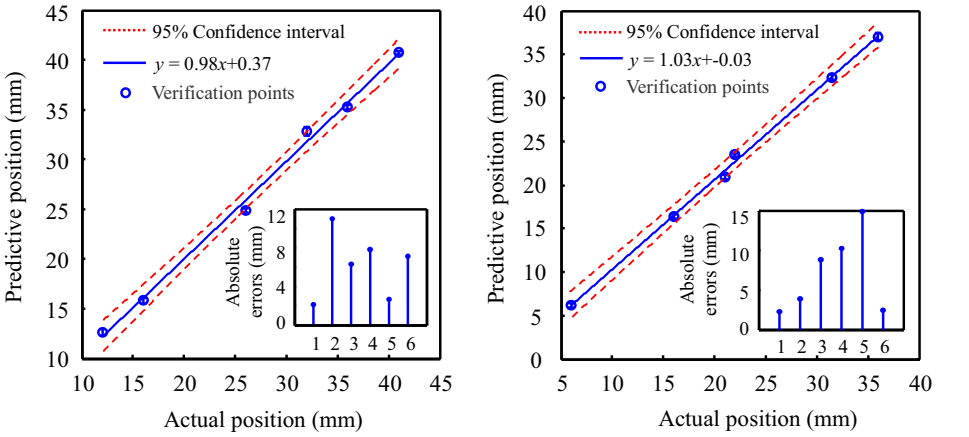

(a) Prediction results of the x coordinates of the verification points

(b) Prediction results of the y coordinates of the verification points

Fig. 9 Linear regression results of six verification points in $[0/90]_{4s}$ fiber laminates

150 kHz, four preamplifiers, the plate, the 2H pencil and 4 preamplifiers. Without additional power supply, the gain preamplification of 20 dB, 40 dB and 60 dB can be selected from the preamplifier. In the experiment, the plate was placed horizontally on the experimental table. High-vacuum grease was added between the sensors and plate surface for a better coupling environment. The signal excitation was performed with a pencil (2H) to simulate the AE source [22]. The tip of the pencil has a circular ring. Under the premise of ensuring the enough length of the pencil core, the same angle between the pencil surface and the plate was maintained to obtain a fixed PLB angle of 30°. At least 8 artificial PLB excitations were performed for each grid node to collect the experimental data.

The AE acquisition software AEwin was selected. Before the experiment, the parameters of AEwin software were set. The threshold value was 40 dB and the gain was 40 dB. The sampling rate was 10 MHz and the pre-trigger was 25.6 μs. The signal length was 2048. The time when the signal first exceeded the threshold value was used to determine the time when the wave arrived at the sensor. The sensor signals received by the 4 channels were derived from the AEwin software to obtain arrival time of the AE signals. Arrival time was read from the acquired AE signal data file. The signal processing algorithm was adopted to localize the AE source.

The localization of AE sources with T-TDM, I-TDM and GRNN-TDM methods was studied in four composite plates with different fiber layers and an aluminum plate with holes. The four anisotropic composite plates with different layups are $[(0/90)_2]_S$, $[0]_{16}$, $[(0/90)_4]_S$, and $[(0/45/90/-45)_2]_S$. The thickness of each layer of the four composite sheets is 0.14 mm. The total thickness of the 16 layers is 2.24 mm and the thickness of the 8 layers is 1.12 mm. The size of the aluminum plate with holes was 50 cm × 80 cm × 0.3 cm. Four holes with the diameters of 2 cm, 3 cm, 5 cm and 10 cm were machined at different positions on the aluminum plate by the laser cutting technology.

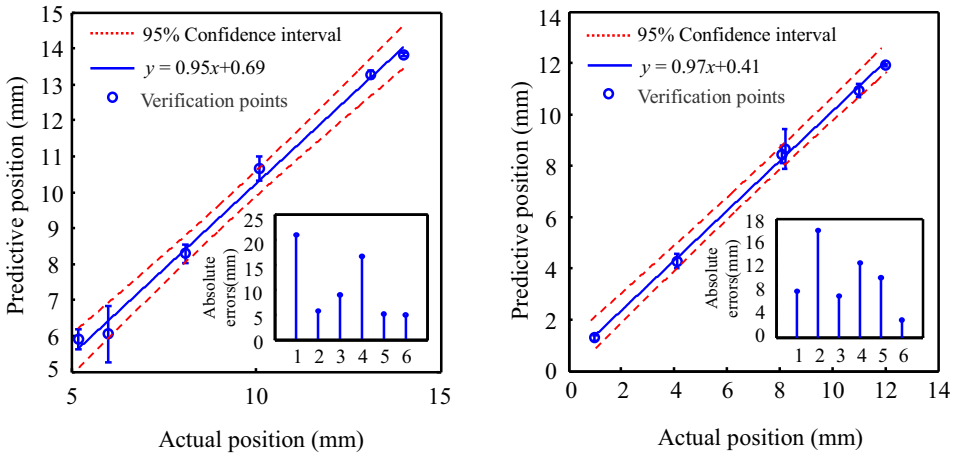

(a) Prediction results of the x coordinates of the verification points

(b) Prediction results of the y coordinates of the verification points

Fig. 10 Linear regression results of six verification points in $[0/90]_{2s}$ fiber laminates

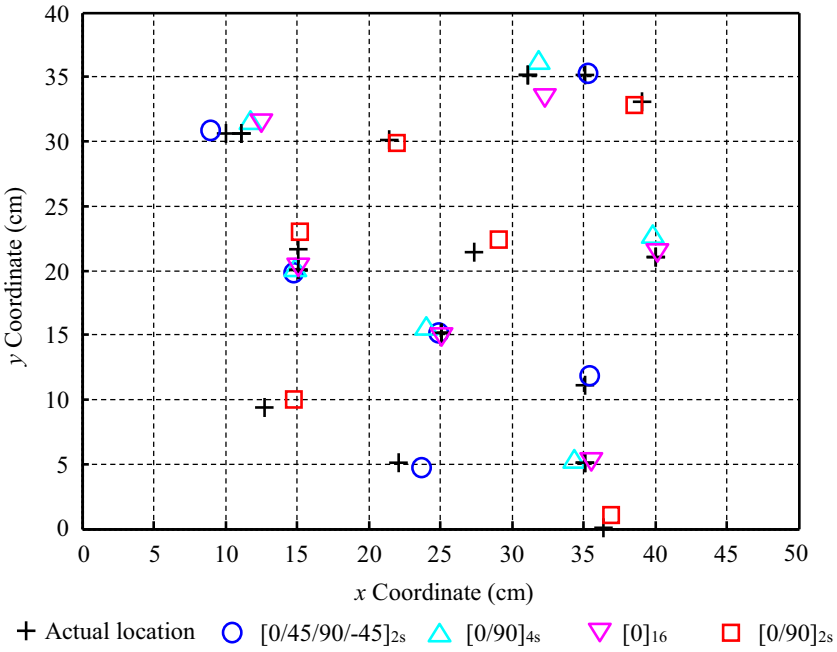

Fig. 11 Source localization results of the GRNN-TDM method in four kinds of composite plates

Results and Discussion

AE Source Localization in Composite Plates

The laminates of the selected composite plates were $[0]_{16}$, $[(0/90)_2]_S$, $[(0/90)_4]_S$ and $[(0/45/90/-45)_2]_S$, respectively. The area of 50 cm × 40 cm was chosen as the detection area and a grid size was set as 5 cm × 5 cm. At least 8 PLB events were conducted at each point.

AE Source Localization Based on T-TDM and I-TDM Methods

Figure 6 shows the average localization errors of the AE source positions in four composite plates by T-TDM and I-TDM methods. Localization errors at each verification point were recorded. Error bands in Fig. 6 indicate a standard deviation related to average localization errors.

The localization errors are shown in Fig. 6. In $[(0/45/90/-45)_2]_S$ fiber layer composite plate, the average localization

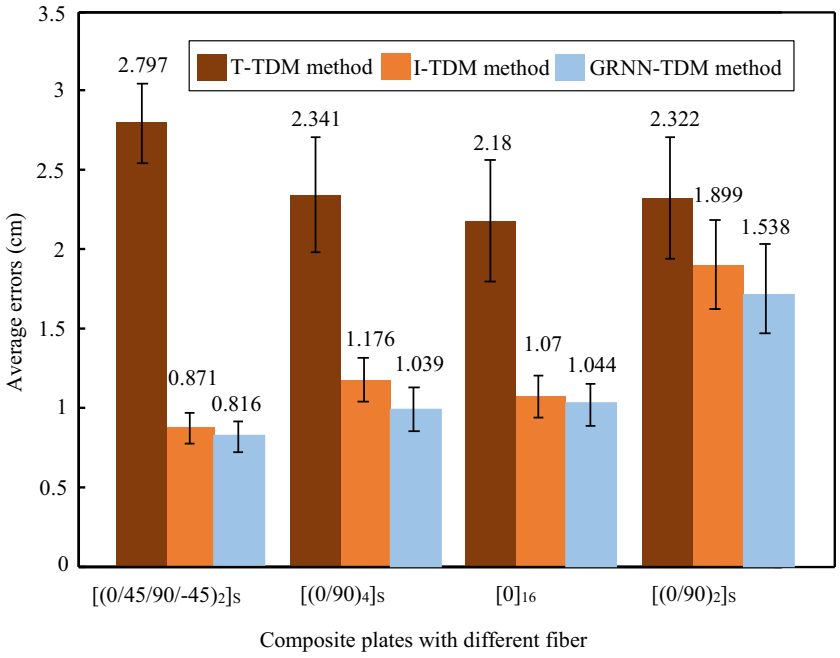

Fig. 12 Average localization errors in four kinds of composite plates of three methods

Table 1 Source localization error statistics based on GRNN-TDM method (unit: cm)

Composite plates	Verification points						Average errors
	1	2	3	4	5	6	
$[(0/45/90/-45)_2]_S$	0.459	0.372	0.325	1.214	1.713	0.816	0.816
$[(0/90)_4]_S$	0.755	0.161	1.988	1.966	0.493	0.875	1.039
$[0]_{16}$	0.322	1.2	1.122	1.331	1.531	0.762	1.044
$[(0/90)_2]_S$	2.334	1.951	1.125	2.113	1.113	0.592	1.538

errors obtained with the T-TDM method and I-TDM method were respectively 2.797 cm and 0.871 cm. In $[(0/90)_4]_S$ fiber layer composite plate, the localization errors obtained with the T-TDM method and I-TDM method were respectively 2.341 cm and 1.176 cm. In $[0]_{16}$ fiber layer composite plate, the localization errors obtained with the T-TDM method and I-TDM method were respectively 2.18 cm and 1.07 cm. In $[(0/90)_2]_S$ fiber layer composite plate, the localization errors obtained with the T-TDM method and I-TDM method were respectively 2.322 cm and 1.899 cm.

AE Source Localization Based on GRNN-TDM Method

In this study, the time difference mapping training data of six pairs of sensor paths collected on the composite plates of four fiber layers were used as the training data. Six verification points were selected to predict the location of AE source in the model established with GRNN-TDM algorithm. The number of the selected sample data was 99. The only setting parameter of GRNN was the spread value (the expansion coefficient of radial basis function). The spread value had a great influence on the accuracy of the prediction model. The greater the spread value was, the smoother the output results were. However, the errors also increased accordingly with the increase in the spread value. Due to the small amount of training data, in order to get a stable and reliable model, in this paper, with cross-validation and loop training methods, the neural network was trained to obtain the best training input data, output data and spread value. The cross-validation method could obtain as much information as possible from the limited training data, so the method was selected in this study. Especially, when learning samples were from multiple directions, the method could effectively avoid the local minimum and overfitting to some extent. The collected training data and verification data were put into the whole data set to verify the localization results of AE source obtained by GRNN-TDM method.

To further analyze the errors of the prediction location of the verification points, the network was used to perform the linear regression analysis with the output of the two parameters of the horizontal and vertical coordinates (x and y) of six verification points and corresponding target vectors. Figure 7, Fig. 8, Fig. 9, and Fig. 10 show the linear regression results of six verification points in four different fiber laminates ($[0]_{16}$, $[(0/90)_2]_S$, $[(0/90)_4]_S$ and $[(0/45/90/-45)_2]_S$) as well as the absolute errors of corresponding locations.

As shown in Fig. 7, Fig. 8, Fig. 9, and Fig. 10, the GRNN-TDM method has the good prediction results of the x-coordinate and y-coordinate of the six verification points in the four composite plates. Prediction results are within the 95% confidence interval and the absolute error of linear regression

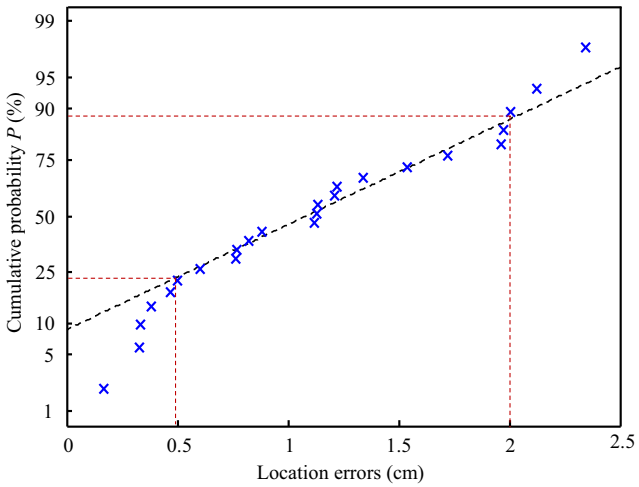

Fig. 13 Error-probability distribution diagram of 24 verification points in composite plates

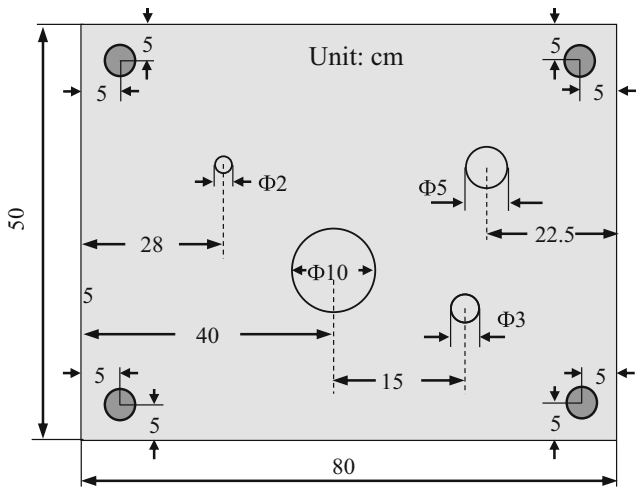

Fig. 14 Aluminum specimen

Table 2 Coordinates of 10 verification points

PLB location	#1	#2	#3	#4	#5	#6	#7	#8	#9	#10
x /cm	6.1	21.6	25.1	35.1	15.1	16.1	32.1	11.1	27.1	5.1
y /cm	6.1	6.6	25.1	16.1	40.1	30.1	35.1	21.1	20.1	35.1

prediction is less than 2 cm. The prediction results are stable and robust, indicating that the output value of the GRNN has a high consistency with the target value. Therefore, the constructed GRNN model can achieve a good prediction result of the defect position in the fiber laminate composite plate. The actual locations of six verification points and the prediction results obtained with the GRNN-TDM method were plotted together. Figure 11 shows the source localization results of the GRNN-TDM method in four composite plates. The localization errors of three methods are shown in Fig. 12.

The predicted results of the verification points with the GRNN-TDM method were obtained and then the Euclidean distance between the predicted results and actual locations of the verification points in four composite plates were calculated. The error analysis of the location at each verification point was performed. Table 1 shows the source localization error statistics of the GRNN-TDM method.

The maximum spacing in the two sensor arrangements on four composite plates is 50 cm. The relative error analysis was performed with the predicted position in Table 1. In $[(0/45/90/-45)_2]_S$ fiber layer composite plate, the average relative localization errors of verification points obtained with T-TDM, I-TDM, and GRNN-TDM methods were respectively 5.6%, 1.7%, and 1.6%. In $[(0/90)_4]_S$ fiber layer composite plate, the average relative localization errors of verification points obtained with T-TDM, I-TDM, and GRNN-TDM methods were respectively 4.7%, 2.4%, and 2.0%. In $[0]_{16}$ fiber layer composite plate, the average relative localization errors of verification points obtained with T-TDM, I-TDM, and GRNN-TDM methods were respectively 4.4%, 2.1%, and 2.0%. In $[(0/90)_2]_S$ fiber layer composite plate, the average relative localization errors of verification points obtained with T-TDM, I-TDM, and GRNN-TDM methods were respectively 4.6%, 3.8%, and 3.0%. The error-probability distribution relationship of 24 verification points of four composite plates is shown in Fig. 13.

The distribution of prediction errors of the 24 verification points obtained with the GRNN-TDM method is described as follows. The prediction errors of 5 verification points are in the range of $x \le 0.5$ cm and the corresponding probability is about 25% or less. The prediction errors of 3 verification points are in the range of $x \ge 2$ cm and the corresponding probability is about 89% or more. The prediction errors of 16 verification points are in the range of 0.5 cm $\le x \le 2$ cm and the corresponding probability is between 25% and 90%. The prediction errors of the verification points obtained with the GRNN-TDM method show a normal probability distribution. AE source localization has the small prediction error and good robustness. The GRNN-TDM method can be used to identify and localize the defects in orthotropic and quasi-

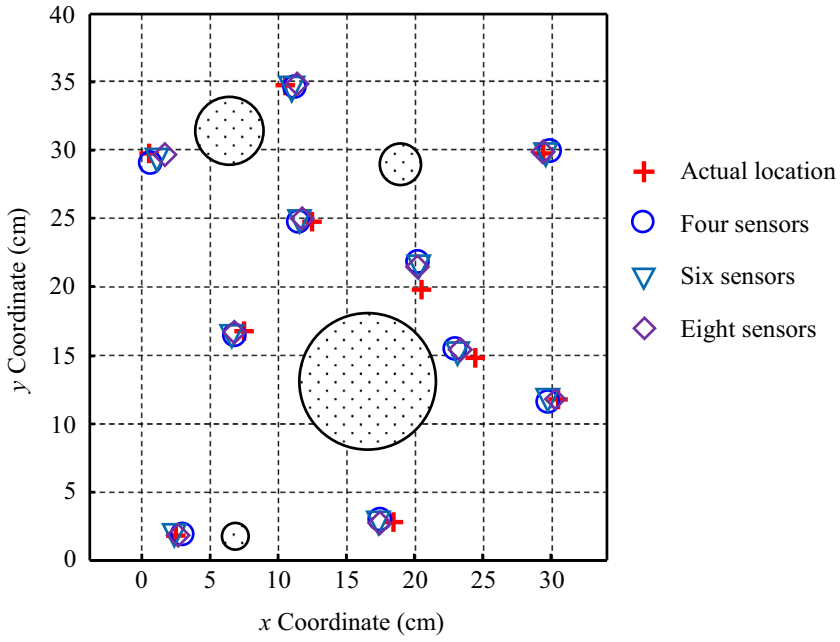

Fig. 15 Localization results obtained with different numbers of sensors

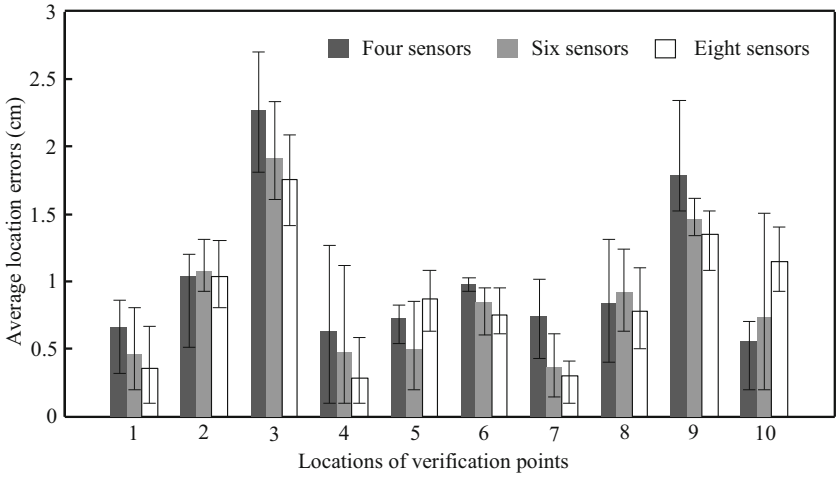

Fig. 16 Verification point errors obtained with different numbers of sensors

isotropic composite plates. Compared with other traditional pattern recognition methods, the GRNN-TDM method showed the higher prediction accuracy in defect localization.

AE Source Localization in an Aluminum Plate with Holes

In plate-like structures, the varying propagation velocity may lead to the inaccurate localization of AE source and defects and holes also affect the propagation path of waves, thus affecting the localization accuracy of AE source. The experimental specimen was an aluminum plate with holes. The size of the plate was 50 cm × 80 cm × 0.3 cm. Four holes with the diameters of 2 cm, 3 cm, 5 cm and 10 cm were machined at different positions on the aluminum plate by laser cutting technology. Four sensors were arranged inside the four corners of the plate. The positions of sensors, the processing sizes and positions of holes are shown in Fig. 14.

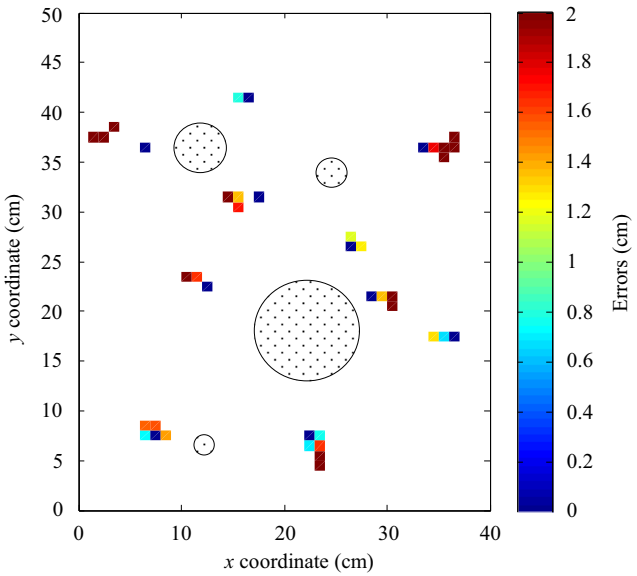

Fig. 17 Imaging of localization results and errors

The coordinates of the 10 verification points are shown in Table 2. Among the selected 10 verification points, the propagation paths of most points such as verification points 2, 3, 6 and 9 need to pass through the holes, but the propagation paths of a small part of the verification points such as the verification point 1 do not pass through the holes. Based on the above analysis, it can be inferred that the experimental points whose propagation paths are interrupted may have large localization errors. The localization errors of the experimental points with uninterrupted propagation paths may be small.

Influence of the Number of Sensors on Localization Results

According to the basic localization principle of the TDM method, the localization of the AE source requires at least three sensors. As the number of sensors increases, the time difference mapping paths also increase largely. In theory, the localization accuracy of AE source increases as the number of sensors increases. Figure 14 shows the influence of the number of sensors on localization results. Localization results of AE source respectively obtained with 4, 6 and 8 sensors are provided.

As shown in Fig. 15, the number of sensors has the less influence on the localization results of 10 verification points. Localization results obtained with different numbers of sensors are similar. Figure 16 shows the error of each verification point obtained with different numbers of sensors. The error bars represent the maximum and minimum errors of each position. The localization errors of the positions 1, 3, 4, 6, 7 and 9 gradually decreased as the number of sensors increased. When the numbers of sensors were respectively 4, 6 and 8, the average localization errors of the 10 verification points were respectively 1.02 cm, 0.87 cm, and 0.86 cm. When the number of sensors was increased to a certain extent, AE source localization accuracy was not significantly improved.

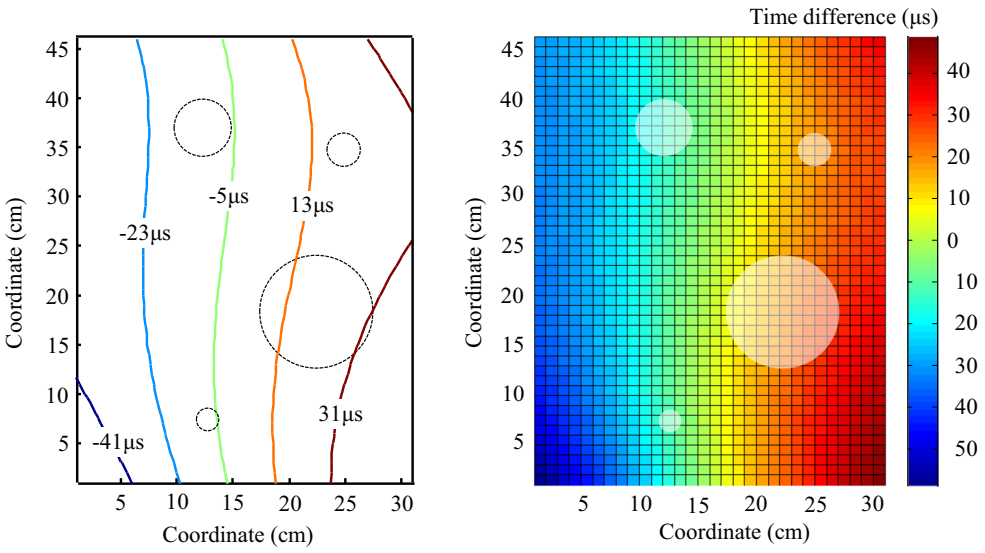

(a) Time difference contour of an aluminum plate with holes

(b) Time difference mapping of an aluminum plate with holes

Fig. 18 Propagation paths of waves and time difference mapping of an aluminum plate with holes

Therefore, 8 sensors were selected in the subsequent verification experiments.

AE Source Localization of an Aluminum Plate with Holes Based on the TDM Method

Firstly, the traditional TOA method was used to localize the acoustic source of the aluminum plate with holes. Figure 17 shows the acoustic source localization results and error imaging images of 10 verification points. The position of the dark blue block in Fig. 16 indicates the actual location of the verification point and the locations of other blocks represent the locations obtained in the 8 repeated experiments. The color depth represents the size of the localization errors.

Figure 18 shows the propagation paths of waves and time difference mapping of aluminum plate with holes. When there are holes in the structure, the wave propagation path is changed, thus affecting the time when the sensor receives the signal. Therefore, the errors of the TOA method are large.

To evaluate the localization performances of different AE source localization algorithms, the T-TDM, I-TDM and GRNN-TDM methods were used to localize and analyze the 10 locations selected in the plate. Figure 19 shows the localization results of AE source in the aluminum plate with holes.

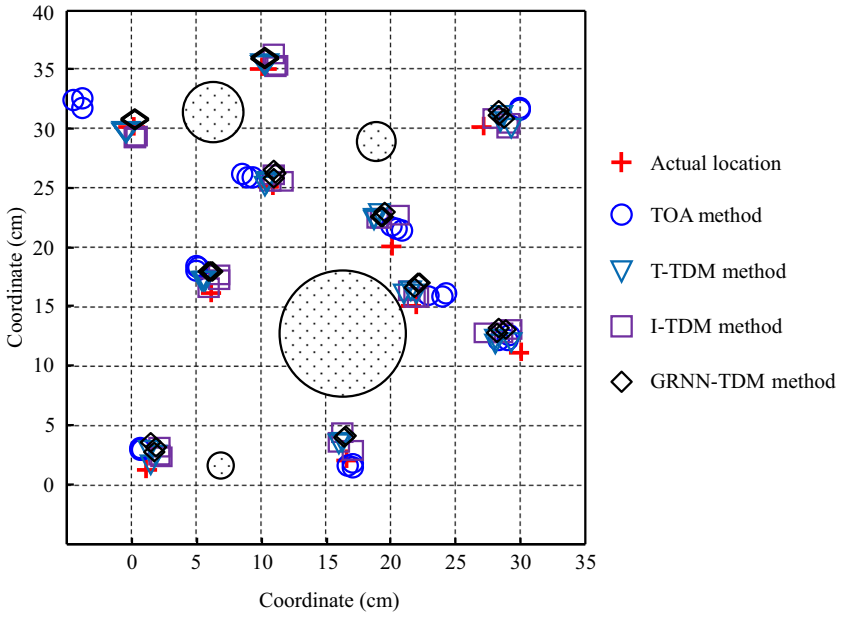

Fig. 19 AE source localization results of an aluminum plate with holes

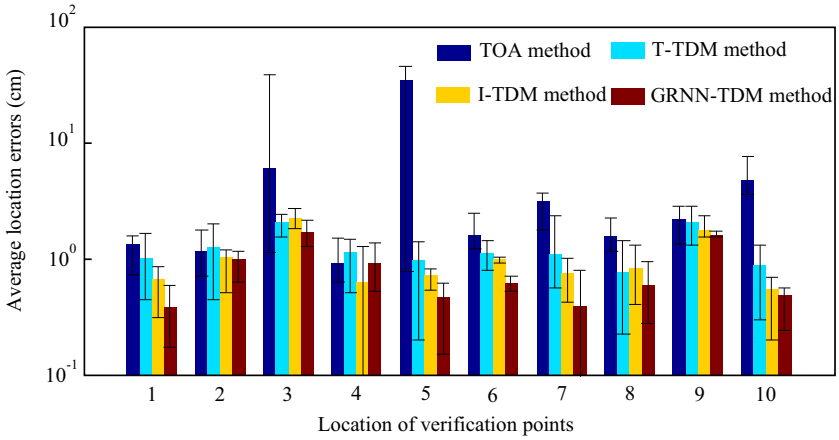

Fig. 20 Average error statistics of AE source localization

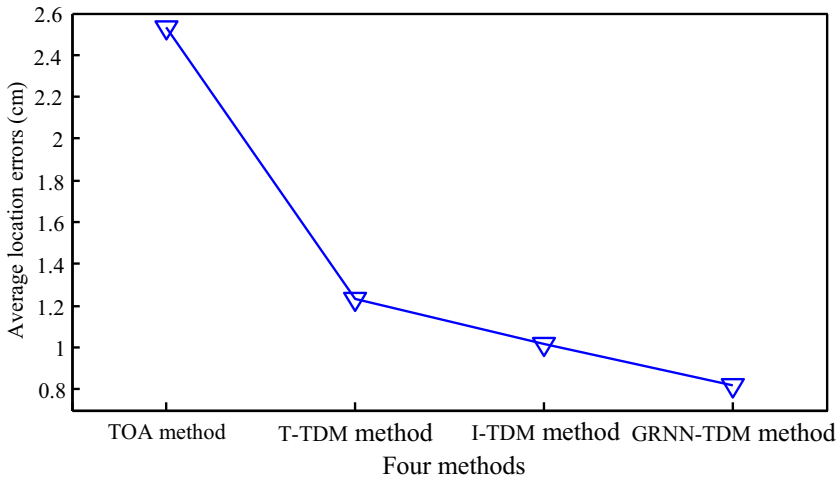

Fig. 21 Average localization errors of different methods

Figure 20 shows the average error statistics of AE source localization. The error bars represent the maximum and minimum errors of corresponding positions. All localization techniques based on TDM methods achieved AE source localization at 10 locations, whereas the TOA method only achieved AE source localization at 9 locations. The localization errors of locations 7 and 10 exceeded 3 cm. For locations 3 and 9, the localization errors obtained with the T-TDM method were respectively 2.06 cm and 2.04 cm because they were close to a hole with a diameter of 100 mm; the localization errors obtained with the I-TDM method were respectively 2.27 cm and 1.78 cm. However, for the entire aluminum plate, the localization errors were only 5.6% and 4.4%, which were much less than 10%. The minimum localization errors obtained with the GRNN method were respectively 0.55 cm and 0.38 cm, which were equivalent to only 1.3% and 0.9% of the overall aluminum plate size.

Figure 21 and Table 3 show the comparison of the average localization errors of different methods. For all verification points, the average localization errors of the TOA, T-TDM, I-TDM and GRNN-TDM methods were 2.01 cm, 1.23 cm, 1.02 cm and 0.82 cm, respectively. Compared with the

Table 3 Average localization errors of different methods

Localization methods	Location errors of verification points (cm)										Average errors (cm)
	#1	#2	#3	#4	#5	#6	#7	#8	#9	#10	
TOA	1.34	1.16	1.33	0.91	34.06	1.63	3.13	1.58	2.22	4.73	2.01
T-TDM	1	1.26	2.06	1.15	0.97	1.11	1.09	0.77	2.04	0.87	1.23
I-TDM	0.66	1.04	2.27	0.63	0.72	0.98	0.74	0.83	1.78	0.55	1.02
GRNN-TDM	0.38	0.99	1.69	0.92	0.47	0.61	0.39	0.59	1.63	0.49	0.82

localization accuracy of the TOA method, the localization accuracies of the T-TDM, I-TDM and GRNN-TDM methods were increased by 38.8%, 49.3% and 59.2%, respectively. The experimental results showed that the I-TDM and GRNN-TDM methods had the largely improved localization performance of all AE source verification points in the plate, indicating the high localization accuracy and reliability.

Conclusions

The AE source localization accuracy is not high due to the dispersion and multi-mode characteristics of wave propagation of the AE signals in plate-like structures, the anisotropy of composite plates, and the discontinuity of wave propagation on aluminum plates with complex geometry. In this paper, with composite plates with different fiber layers and an aluminum plate with holes as the research objects, based on T-TDM and I-TDM methods, GRNN-TDM method was proposed to predict AE source location.

The T-TDM and I-TDM methods could quickly and accurately localize the AE source in the structure without considering the propagation speed of the wave and the mode. Compared with the T-TDM method, the I-TDM method used unsupervised clustering to select the correct AE events and eliminate abnormal data caused by artificial or environmental factors. Then the minimum difference method was used to calculate the AE source location. The GRNN-TDM method avoided the problem of optimal cluster diameter selection in T-TDM method and improved the localization accuracy.

Compared with the T-TDM and I-TDM methods, the GRNN-TDM method not only reduced the workload, but also improved the localization accuracy of the AE source and the generality of the algorithm. The GRNN-TDM method was used to predict the locations of verification points in composite plates with different fiber layers. The errors were within the 95% confidence interval and the total recognition rate was above 95%. The location prediction errors of 24 verification points showed the normal probability distribution. The verification results were obviously improved and the localization accuracy obtained with the GRNN-TDM method was better than that obtained with the T-TDM and I-TDM methods.

The AE source localization study on the aluminum plate with holes was experimentally carried out with 4, 6 and 8 sensors, respectively. The number of sensors was positively correlated with the localization accuracy of AE source. As the number of sensors increased, the localization accuracy increased. Compared with the localization accuracy of the TOA method, the localization accuracies of the T-TDM, I-TDM and GRNN methods were greatly improved by 38.8%, 49.3% and 59.2%, respectively. The GRNN-TDM method had the higher localization accuracy on the aluminum plate with holes than the other three methods.

In the study, AE source generated by PLB was explored, but the actual AE source generated in the process of cyclic fatigue and fiber breakage was not investigated. Different types of real AE sources affected AE source localization. Therefore, the AE source localization errors and its influencing factors in industrial applications will be further explored.

Acknowledgments This work was supported by the National Key R&D Program of China (Grant No. 2018YFC0809003) and the National Natural Science Foundation of China (Grant No. 11772014).

References

1. Achenbach JD (2009) Structural health monitoring–what is the prescription. Mech Res Commun 36(2):137–142
2. Farrar CR, Worden K (2007) An introduction to structural health monitoring. Philosophical Trans Royal Soc London A: Mathematical, Phys Eng Sci 365(1851):303–315
3. Sohn H, Farrar CR, Hemez FM, Shunk DD, Stinemates DW, Nadler BR. A review of structural health monitoring literature: 1996-2001. Los Alamos National Laboratory Report, 2004
4. Kaphle Manindra (2012) Analysis of acoustic emission data for accurate damage assessment for structural health monitoring applications. Ph.D. dissertation of Queensland University of Technology, Brisbane
5. Miller RK, Hill EK, Moore PO (2005) Non-destructive testing handbook, 3rd edn, vol. 6, Acoustic emission testing. American Society for Nondestructive Testing, Ohio
6. Baxter MG, Pullin R, Holford KM et al (2007) Delta T source location for acoustic emission. Mech Syst Signal Process 21(3): 1512–1520
7. Kundu T (2014) Acoustic source localization. Ultrasonics 54:25–38
8. Tobias A (1976) Acoustic-emission source location in two dimensions by an array of three sensors. Non-Destructive Testing 9(1):9–12
9. Mhamdi L, Schumacher T (2015) A comparison between time-of-arrival and novel phased array approaches to estimate acoustic emission source locations in a steel plate. J Nondestruct Eval 34(4):1–13
10. Kundu T, Nakatani H, Takeda N (2012) Acoustic source localization in anisotropic plates. Ultrasonics 52(6):740–746
11. Nakatani H, Kundu T, Takeda N (2014) Improving accuracy of acoustic source localization in anisotropic plates. Ultrasonics 54(7):1776–1788
12. Kundu T, Yang X, Nakatani H, Takeda N (2015) A two-step hybrid technique for accurately localizing acoustic source in anisotropic structures without knowing their material properties. Ultrasonics 56:271–278
13. Park WH, Packo P, Kundu T (2017) Acoustic source localization in an anisotropic plate without knowing its material properties–a new approach. Ultrasonics 79:9–17
14. Sen N, Kundu T (2018) A new wave front shape-based approach for acoustic source localization in an anisotropic plate without knowing its material properties. Ultrasonics 87:20–32
15. Sen N, Gawroński M, Packo P, Uhl T, Kundu T. Acoustic source localization in anisotropic plates without knowing their material properties: An experimental investigation. Proceedings of SPIE - The International Society for Optical Engineering, 2019, 10972: 1097224-1-19. Health Monitoring of Structural and Biological Systems XIII 2019, March 4, 2019 - March 7, 2019
16. Simone MED, Ciampa F, Boccardi S, MeoImpact M (2017) Source localisation in aerospace composite structures. Smart Mater Struct 26(12):125026

17. Ebrahimkhanlou A, Salamone S (2017) Acoustic emission source localization in thin metallic plates: a single-sensor approach based on multimodal edge reflections. Ultrasonics 78:134–145
18. Ebrahimkhanlou A, Dubuc B, Salamone S (2019) A generalizable deep learning framework for localizing and characterizing acoustic emission sources in riveted metallic panels. Mech Syst Signal Process 130:248–272
19. Liu ZH, Dong TC, Peng QL, He CF, Li QF, Wu B (2018) AE source localization in a steel plate with the dispersive A_0 mode based on the cross-correlation technique and time reversal principle. Mater Eval 76(3):371–382
20. James C, John L, Mark S (1998) Neural network approach to locating acoustic emission sources in nondestructive evaluation. Proc Am Control Conference, Philadelphia:68–72
21. Eaton MJ, Pullin R, Holford KM (2012) Acoustic emission source location in composite materials using Delta T mapping. Composites Part A 43(6):856–863
22. Hsu NN, Breckenridge FR (1981) Characterization and calibration of acoustic emission sensors. Mater Eval 39:60–68
23. Scholey JW, Wisnom PD, Friswell MR, Pavier MI, Alika MJ (2009) MR, a generic technique for acoustic emission source location. J Acoust Emiss 27:291–298